Surrogate Mass Optimization for Helicopter Vibration Tests

Lennart Frie[1] , **Oliver Dieterich**[2] , **Peter Eberhard**[1]

[1] Institute of Engineering and Computational Mechanics, University of Stuttgart
Pfaffenwaldring 9, 70569 Stuttgart, Germany
lennart.frie@itm.uni-stuttgart.de
peter.eberhard@itm.uni-stuttgart.de

[2] Airbus Helicopters Germany GmbH
Dynamics and Vibrations
Industriestr. 4, 86607 Donauwörth, Germany
oliver.dieterich@airbus.com

ABSTRACT

In helicopter dynamics, the identification of eigenmodes and eigenfrequencies is an important issue to predict and prevent vibrations of the airframe. In ground vibration tests, a surrogate mass is typically coupled to the rotor mast to substitute the rotating rotor. Currently, the choice of the amount of this mass is based on expert knowledge and experience, but there is no general procedure. This work presents a novel approach to select the amount of the surrogate mass in dependence on the frequency that is to be investigated. For this purpose, a modal reference solution is created from the coupled multibody system and a parametrically reduced surrogate model with a lumped mass is set up. An adequate amount of the mass is determined by optimizing the mode shapes and eigenfrequencies of the surrogate model with respect to the reference. To this end, a very efficient and accurate parametric reduced order model is generated with Krylov subspaces that significantly reduces the numerical costs for evaluations of the objective function. By minimizing this objective function, which describes the deviation of eigenfrequencies and eigenmodes, different optimal masses are identified for different frequencies that move the modal characteristics of the surrogate model closer to the reference.

Keywords: Parametric Model Order Reduction, Elastic Multibody System, Modal Analysis, Helicopter Dynamics, Surrogate Modeling

1 INTRODUCTION

Helicopters are very lightweight and flexible structures, making them prone to vibrations. In product development and production, the simulative and experimental prediction of eigenfrequencies and eigenmodes, especially near the rotor harmonics and blade passage frequency, is of great importance to prevent unwanted vibrations, potentially causing discomfort for the pilot and passengers. The eigenfrequencies can be determined with an experimental modal analysis which is also called ground vibration test in aerospace engineering. A common problem with the experimental test setup is that the coupled elastic multibody system (EMBS), consisting of the elastic airframe and the elastic rotating main rotor, behaves differently from the free airframe. Hence, it is not sufficient to consider only the free airframe. It is also not practically, though, to include the rotating rotor in the experimental setup of ground vibration tests.

In industrial practice, the behavior of the coupled system is approximated by coupling surrogate masses to the rotor shaft, see, e.g., [1]. However, the choice of the amount of mass is not trivial and there is no general procedure to determine an adequate surrogate mass. As yet, the choice is based on experience and expert knowledge. This paper aims to overcome this issue and presents a novel approach for selecting a surrogate mass that optimally approximates a particular eigenmode of the coupled system. A reference eigensolution is computed for the EMBS with an elastic airframe and a geometrically stiffened elastic rotor. The amount of the surrogate mass is then determined by optimizing the eigenfrequencies and eigenmodes of the surrogate model, where the rotor is not included, with respect to the reference. The airframe model is reduced with parametric model

order reduction (PMOR) techniques, whereby efficient system evaluations and, consequently, optimization of the surrogate model under varying lumped mass are enabled.

This paper is organized as follows. After this introduction, in Section 2, the most important theoretical backgrounds on EMBS and PMOR are revised. In Section 3 it is then shown, how the reference model is built. Section 4 deals with the design and optimization of the surrogate model. Important results are presented in Section 5 and a short conclusion with some outlooks is finally given in Section 6.

2 THEORETICAL BACKGROUND

This section briefly reviews the main theoretical backgrounds on EMBS with rotating bodies and PMOR.

2.1 Elastic multibody systems with rotating bodies

Mechanical systems are often divided into different components that interact with each other. A popular method to describe such systems is the floating frame of reference (FFR) approach described in [2]. Its idea is to separate large nonlinear described rigid body motions from small linear-elastic deformations. The equation of motion of a free body described with the FFR reads

$$\begin{bmatrix} m\boldsymbol{I} & m\tilde{\boldsymbol{c}}^\top & \boldsymbol{C}_\mathrm{t}^\top \\ m\tilde{\boldsymbol{c}} & \boldsymbol{J} & \boldsymbol{C}_\mathrm{r}^\top \\ \boldsymbol{C}_\mathrm{t} & \boldsymbol{C}_\mathrm{r} & \boldsymbol{M}_\mathrm{e} \end{bmatrix} \begin{bmatrix} \dot{\boldsymbol{v}} \\ \dot{\boldsymbol{\omega}} \\ \ddot{\boldsymbol{q}} \end{bmatrix} = \begin{bmatrix} \boldsymbol{h}_{\omega\mathrm{t}} + \boldsymbol{h}_{\mathrm{gt}} + \boldsymbol{h}_{\mathrm{pt}} + \boldsymbol{h}_{\mathrm{dt}} \\ \boldsymbol{h}_{\omega\mathrm{r}} + \boldsymbol{h}_{\mathrm{gr}} + \boldsymbol{h}_{\mathrm{pr}} + \boldsymbol{h}_{\mathrm{dr}} \\ \boldsymbol{h}_{\omega\mathrm{e}} + \boldsymbol{h}_{\mathrm{ge}} + \boldsymbol{h}_{\mathrm{pe}} + \boldsymbol{h}_{\mathrm{de}} \end{bmatrix} + \begin{bmatrix} \boldsymbol{0} \\ \boldsymbol{0} \\ -\boldsymbol{k}_\mathrm{e} \end{bmatrix}. \tag{1}$$

Here, $\boldsymbol{v}$ and $\boldsymbol{\omega}$ are the rigid body translational and angular velocity, m is the mass of the body, $\boldsymbol{I}$ is the identity, $\boldsymbol{J}$ is the inertia tensor, $\tilde{\boldsymbol{c}}$ is a skew-symmetric matrix that describes the location of the center of mass, $\boldsymbol{C}_\mathrm{t}$, $\boldsymbol{C}_\mathrm{r}$ are coupling matrices, and $\boldsymbol{M}_\mathrm{e} \in \mathbb{R}^{N\times N}$ is the elastic mass matrix with N elastic degrees of freedom. The indices $\bullet_\mathrm{t}$, $\bullet_\mathrm{r}$ and $\bullet_\mathrm{e}$ denote translational, rotational and elastic degrees of freedom, respectively, and the notations $\dot{\bullet} := {}^{\mathrm{d}\bullet}/_{\mathrm{d}t}$ and $\ddot{\bullet} := {}^{\mathrm{d}^2\bullet}/_{\mathrm{d}t^2}$ are used for the time derivatives in this paper. The right-hand terms in Equation (1) are inertia forces $\boldsymbol{h}_\omega$, gravity forces $\boldsymbol{h}_\mathrm{g}$, surface loads $\boldsymbol{h}_\mathrm{p}$, external forces $\boldsymbol{h}_\mathrm{d}$ and internal forces

$$\boldsymbol{k}_\mathrm{e} = (\boldsymbol{K}_\mathrm{geo}(\boldsymbol{\omega}) + \boldsymbol{K}_\mathrm{e})\boldsymbol{q} + \boldsymbol{D}_\mathrm{e}\dot{\boldsymbol{q}}. \tag{2}$$

The linear-elastic deformation of an undamped body without translational rigid body degrees of freedom (dof) ($\dot{\boldsymbol{v}} = \boldsymbol{v} = \boldsymbol{0}$), without surface loads ($\boldsymbol{h}_\mathrm{pe} = \boldsymbol{0}$), and with neglection of gravity forces that are often small compared to other acting forces ($\boldsymbol{h}_\mathrm{ge} = \boldsymbol{0}$), is described by

$$\boldsymbol{M}_\mathrm{e}\ddot{\boldsymbol{q}} + \boldsymbol{K}_\mathrm{e}\boldsymbol{q} = \boldsymbol{h}_\mathrm{de}, \tag{3}$$

if the body does not rotate, and by

$$\boldsymbol{M}_\mathrm{e}\ddot{\boldsymbol{q}} + \left[\boldsymbol{K}_\mathrm{geo}(\boldsymbol{\omega}) + \boldsymbol{K}_\mathrm{e}\right]\boldsymbol{q} = \boldsymbol{h}_{\omega\mathrm{e}} + \boldsymbol{h}_\mathrm{de}, \tag{4}$$

if it rotates. For a constant rotation about the z-axis with $\boldsymbol{\omega} = [0,0,\Omega]^\top$ and $\dot{\boldsymbol{\omega}} = \boldsymbol{0}$, and with the separation of the inertia forces

$$\boldsymbol{h}_{\omega e} = \boldsymbol{h}_{\omega\mathrm{e}0} + \boldsymbol{h}_{\omega\mathrm{e}1}(\boldsymbol{q},\dot{\boldsymbol{q}}) = \boldsymbol{h}_{\omega\mathrm{e}0} - 2\Omega\boldsymbol{G}\dot{\boldsymbol{q}} - \Omega^2\boldsymbol{K}_\mathrm{soft}\boldsymbol{q}, \tag{5}$$

Equation (4) can be rewritten to

$$\boldsymbol{M}_\mathrm{e}\ddot{\boldsymbol{q}} + 2\Omega\boldsymbol{G}\dot{\boldsymbol{q}} + \left[\boldsymbol{K}_\mathrm{e} + \Omega^2(\boldsymbol{K}_\mathrm{geo} + \boldsymbol{K}_\mathrm{soft})\right]\boldsymbol{q} = \boldsymbol{h}_\mathrm{de}. \tag{6}$$

The constant mass and stiffness matrices $\boldsymbol{M}_\mathrm{e}$ and $\boldsymbol{K}_\mathrm{e}$ result from the linear finite element method and the gyroscopic matrix $\boldsymbol{G}$ and the softening matrix $\boldsymbol{K}_\mathrm{soft}$ can be computed with inertia shape

integrals from standard input data (SID), see [3]. The derivation of the geometric stiffness matrix $\boldsymbol{K}_{\mathrm{geo}}$, instead, requires a little more effort. A detailed and complete derivation of the different terms is provided in [2, 4] and their underlying effects in the context of helicopter rotor dynamics are extensively investigated in [5].

The geometric stiffness matrix can in principle also be computed from ansatz functions, but finite element solvers usually do not provide them to the user and, thus, another approach has to be used to obtain them as also explained in [6, 7]. The centrifugal force $\boldsymbol{h}_{\omega\mathrm{e}0}$ acting on the body is computed with the multibody tool Neweul-M^2. This force can then be applied to the flexible body to find the geometric stiffness matrix in a quasi-static analysis. The equilibrium of the equation $\boldsymbol{K}_{\mathrm{T}}\boldsymbol{q} = \boldsymbol{h}_{\omega\mathrm{e}0}$ containing the tangential stiffness matrix $\boldsymbol{K}_{\mathrm{T}} = \boldsymbol{K}_{\mathrm{e}} + \Omega^2\boldsymbol{K}_{\mathrm{geo}}$ is determined by updating the stiffness matrix iteratively with a nonlinear static finite element solver. In this work, the solver SOL106 of MSC Nastran, see[8], is used on that account.

2.2 Parametric model order reduction

For better readability, the index $\bullet_{\mathrm{e}}$ is omitted from here on, but it is always referred to the elastic part of Equation (1). The accurate modeling of complex mechanical systems and the increasing demand for details usually leads to a fine discretization of the flexible bodies and, hence, the dimension of this elastic part is naturally high. Despite ever-increasing computational power, these high-dimensional systems cannot be evaluated in a reasonable amount of time, which is, however, a necessary requirement for many tasks such as optimization. Efficient evaluations are only possible through model order reduction (MOR) whereby the full model is approximated with a reduced model that has much less dof, $n \ll N$. In this paper, only non-rotating bodies are reduced. A parametric reduction approach for rotating bodies is presented in [7].

In order to apply projection-based MOR, the external forces are written as matrix-vector product $\boldsymbol{h}_{\mathrm{d}} = \boldsymbol{B}\boldsymbol{u}$ and system outputs are extracted with $\boldsymbol{y} = \boldsymbol{C}\boldsymbol{q}$. This leads to the second-order input-output system

$$\begin{aligned} \boldsymbol{M}\ddot{\boldsymbol{q}} + \boldsymbol{K}\boldsymbol{q} &= \boldsymbol{B}\boldsymbol{u}, \\ \boldsymbol{y} &= \boldsymbol{C}\boldsymbol{q}. \end{aligned} \tag{7}$$

The matrices $\boldsymbol{B} \in \mathbb{R}^{N\times b}$ and $\boldsymbol{C} \in \mathbb{R}^{c\times N}$ are the input and output matrices of the system. The vectors $\boldsymbol{u} \in \mathbb{R}^b$ and $\boldsymbol{y} \in \mathbb{R}^c$ are the inputs and outputs. The basic idea of projection-based MOR is to approximate the state vector within a subspace $\mathscr{V} = \mathrm{span}\{\boldsymbol{V}\} \subset \mathbb{R}^n$ by

$$\boldsymbol{q} \approx \boldsymbol{V}\tilde{\boldsymbol{q}}, \qquad \dim(\boldsymbol{q}) = N \gg \dim(\tilde{\boldsymbol{q}}) = n \qquad \text{and} \qquad \boldsymbol{V} \in \mathbb{R}^{N\times n}. \tag{8}$$

Plugging Equation (8) into Equation (7) and left-multiplying by $\boldsymbol{V}^\top$ leads to the reduced system

$$\begin{aligned} \tilde{\boldsymbol{M}}\ddot{\tilde{\boldsymbol{q}}} + \tilde{\boldsymbol{K}}\tilde{\boldsymbol{q}} &= \tilde{\boldsymbol{B}}\boldsymbol{u}, \\ \tilde{\boldsymbol{y}} &= \tilde{\boldsymbol{C}}\tilde{\boldsymbol{q}}. \end{aligned} \tag{9}$$

The tilde indicates quantities of the reduced model. Its quite small system matrices result from

$$\tilde{\boldsymbol{M}} = \boldsymbol{V}^\top\boldsymbol{M}\boldsymbol{V}, \quad \tilde{\boldsymbol{K}} = \boldsymbol{V}^\top\boldsymbol{K}\boldsymbol{V}, \quad \tilde{\boldsymbol{B}} = \boldsymbol{V}^\top\boldsymbol{B}, \quad \tilde{\boldsymbol{C}} = \boldsymbol{C}\boldsymbol{V}. \tag{10}$$

There are different methods to build the projection matrix $\boldsymbol{V}$. Two methods that are used in this work are briefly explained in the following.

An intuitive and probably the most frequently used method to span the subspace $\mathscr{V}$ is modal truncation. There, the first n eigenmodes $\boldsymbol{\phi}_i, i = 1,\ldots,n$ of the system are calculated and used to span the subspace with

$$\boldsymbol{V} = [\boldsymbol{\phi}_1, \boldsymbol{\phi}_2, \ldots, \boldsymbol{\phi}_n]. \tag{11}$$

Another method, which has gained popularity over the last few years, is moment matching with Krylov subspaces, see [9] and [10] for the application to helicopters. It aims at approximating the transfer function $\boldsymbol{H}(s) = \boldsymbol{C}\left(s^2\boldsymbol{M}+\boldsymbol{K}\right)^{-1}\boldsymbol{B}$ of the system, where s is the Laplace variable. Therefore, the transfer function is written as a power series around expansion points s_k, which are also called shifts. An equidistant distribution of the shifts in the frequency band of interest often leads to sufficiently good results. Advanced shift selection methods are, e.g., shown in [11] and [12]. At these shifts, the first J_k moments are matched implicitly by the use of Krylov subspaces. Choosing the projection matrix for $J_k = 1$ with

$$\operatorname{span}(\boldsymbol{V}) = \operatorname{span}\left[\ (\sigma_1^2\boldsymbol{M}+K)^{-1}\boldsymbol{B},\quad \ldots,\quad (\sigma_\nu^2\boldsymbol{M}+\boldsymbol{K})^{-1}\boldsymbol{B}\ \right] \tag{12}$$

for $k = 1,\ldots,\nu$ ensures $\boldsymbol{H}(\sigma_k) = \tilde{\boldsymbol{H}}(\sigma_k)$ and for $\boldsymbol{C} = \boldsymbol{B}^{\mathrm{T}}$ also $\frac{\partial \boldsymbol{H}(\sigma_k)}{\partial s} = \frac{\partial \tilde{\boldsymbol{H}}(\sigma_k)}{\partial s}$, as [13] shows.

Mechanical systems often depend on parameters $\boldsymbol{p} \in \mathscr{P}$. If these parameters shall be optimized with regard to a performance function, a reduced model is required that is efficient to evaluate and that can adequately represent the parameter dependency of the full model because many system evaluations at different $\boldsymbol{p}$ are necessary during optimization. This can be achieved with PMOR. We now consider the parametric system

$$\begin{aligned} \boldsymbol{M}(p)\ddot{\boldsymbol{q}} + \boldsymbol{K}(p)\boldsymbol{q} &= \boldsymbol{B}(p)\boldsymbol{u}, \\ \boldsymbol{y} &= \boldsymbol{C}(p)\boldsymbol{q} \end{aligned} \tag{13}$$

which is equal to Equation (7) but depends on a parameter p. The parameter p in general does not require to be one-dimensional, but we do not need multidimensional parameter spaces in the scope of this paper. The global reduction matrix $\boldsymbol{V}_{\mathrm{G}}$ for a convex parameter space $\mathscr{P} = [p_{\min}, p_{\max}]$ can be built by reducing the full system at a selection of discrete parameter samples $p_i \in \mathscr{P}$ with $i = 1,\ldots,d$. The global subspace is then spanned by composing the different projection matrices to $\boldsymbol{V}_{\mathrm{G}} = [\boldsymbol{V}_1,\ldots,\boldsymbol{V}_d] \in \mathbb{R}^{N\times dn}$.

2.3 Comparative measures

In order to compare different models, some measures are introduced that relate one model to another. In the frequency domain, the relative error

$$\varepsilon(s) = \frac{\|\boldsymbol{H}(s) - \tilde{\boldsymbol{H}}(s)\|_F}{\|\boldsymbol{H}(s)\|_F} \tag{14}$$

of the Frobenius norm $\|\bullet\|_{\mathrm{F}}$ of the transfer matrix is a widely spread measure. Furthermore, the i-th eigenfrequency of a reference model $f_{\mathrm{ref},i}$ and the j-th eigenfrequency of a test model $f_{\mathrm{test},j}$ can be compared by their squared relative difference

$$\Delta f = \left(\frac{f_{\mathrm{ref},i} - f_{\mathrm{test},j}}{f_{\mathrm{ref},i}}\right)^2. \tag{15}$$

The compliance of the related eigenmodes ϕ is typically measured with the modal assurance criterion (MAC)

$$\mathrm{MAC}_{ij}(m) = \frac{\left|\boldsymbol{\phi}_{\mathrm{ref},i}^{\mathrm{H}}\boldsymbol{\phi}_{\mathrm{test},j}\right|^2}{\left(\boldsymbol{\phi}_{\mathrm{ref},i}^{\mathrm{H}}\boldsymbol{\phi}_{\mathrm{ref},i}\right)\left(\boldsymbol{\phi}_{\mathrm{test},j}^{\mathrm{H}}\boldsymbol{\phi}_{\mathrm{test},j}\right)}. \tag{16}$$

3 COUPLED REFERENCE SOLUTION

The goal of this work is to fit a surrogate model to a reference solution and, thus, at first a reference solution is needed. Since in this case, no measurement is available that can serve as a reference, a reference model is built, which describes the coupled system of the airframe and the rotating rotor. Mode shapes and related frequencies are computed for this model that consists of an elastic airframe with 281 992 dof and a geometrically stiffened rotor with 3721 dof. The rotor consists of five equal blades and a rigid hub. Quantities belonging to the airframe, to the rotor, to a blade, and to the coupled systems are indicated with superscripts $\bullet^{\mathrm{A}}$, $\bullet^{\mathrm{R}}$, $\bullet^{\mathrm{B}}$, and $\bullet^{\mathrm{CS}}$ in the following.

3.1 Coupling of rotor and airframe

The calculation of the rotation-dependent terms yields the equation of motion of the clamped, stiffened rotor blade described in with blade coordinates $\boldsymbol{q}_{\mathrm{c}}^{\mathrm{B}} \in \mathbb{R}^{N_{\mathrm{c}}^{\mathrm{B}}}$, where $N_{\mathrm{c}}^{\mathrm{B}} = N^{\mathrm{B}} - 6$ and where N^{B} is the number of degrees of freedom of the free blade. The blade is decoupled by considering inertia cross-coupling effects and the rigid body parent degrees of freedom $\boldsymbol{q}_{\mathrm{p}}^{\mathrm{B}} \in \mathbb{R}^{6}$ at the coupling node. The equation of motion of the free blade results from

$$\begin{bmatrix} \boldsymbol{M}_{\mathrm{r}}^{\mathrm{B}} & \boldsymbol{L}^{\top} \\ \boldsymbol{L} & \boldsymbol{M}^{\mathrm{B}} \end{bmatrix} \begin{bmatrix} \ddot{\boldsymbol{q}}_{\mathrm{p}}^{\mathrm{B}} \\ \ddot{\boldsymbol{q}}_{\mathrm{c}}^{\mathrm{B}} \end{bmatrix} + \begin{bmatrix} \boldsymbol{0} & \boldsymbol{0} \\ \boldsymbol{0} & \boldsymbol{K}^{\mathrm{B}} \end{bmatrix} \begin{bmatrix} \boldsymbol{q}_{\mathrm{p}}^{\mathrm{B}} \\ \boldsymbol{q}_{\mathrm{c}}^{\mathrm{B}} \end{bmatrix} = \begin{bmatrix} \boldsymbol{h}_{\mathrm{r}}^{\mathrm{B}} \\ \boldsymbol{h}^{\mathrm{B}} \end{bmatrix} \tag{17}$$

with the rigid body mass matrix $\boldsymbol{M}_{\mathrm{r}}^{\mathrm{B}} \in \mathbb{R}^{6\times 6}$. The matrix $\boldsymbol{L}$ is defined as $\boldsymbol{L} = \boldsymbol{\Phi}_{\mathrm{r}}^{\mathrm{B}} \boldsymbol{M}^{\mathrm{B}}$ and provides the off-diagonal coupling terms between parent states and elastic states, see [14] and [15] for the application to helicopter dynamics. The matrix $\boldsymbol{\Phi}_{\mathrm{r}}^{\mathrm{B}} \in \mathbb{R}^{6\times N_{\mathrm{c}}^{\mathrm{B}}}$ contains the translational and rotational rigid body modes. The states of the free blade are then $\boldsymbol{q}^{\mathrm{B}} = [\boldsymbol{q}_{\mathrm{p}}^{\mathrm{B}}, \boldsymbol{q}_{\mathrm{c}}^{\mathrm{B}}]^{\top}$.

The free blades can now be coupled to obtain the free rotor. The rotor is attached to the airframe with algebraic constraints in all translational dof and the rotational dof around the pitch and the roll axis. The coupled system, visualized in Figure 1, has $N^{\mathrm{CS}} = N^{\mathrm{A}} + N^{\mathrm{B}} - 5$ degrees of freedom and is described by minimal coordinates $\boldsymbol{q}^{\mathrm{CS}} \in \mathbb{R}^{N^{\mathrm{CS}}}$.

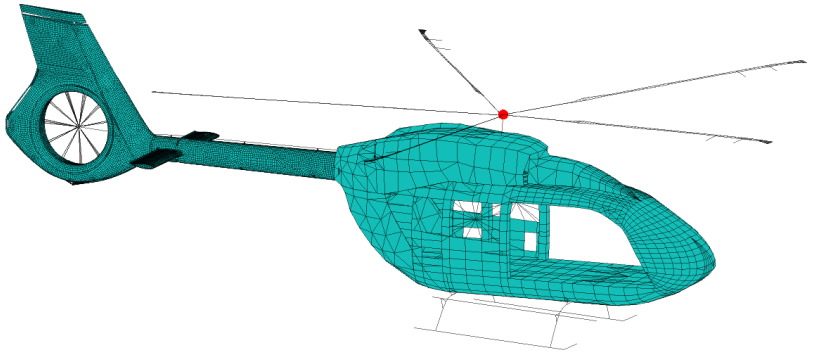

Figure 1: Coupled Finite Element Model with marked coupling node of twin-engine light helicopter and a five-bladed bearingless main rotor system used at Airbus Helicopters.

3.2 Selection of relevant airframe modes

From the coupled system those modes and frequencies must be extracted that shall be approximated when using a surrogate rotor mass. First, the dof that belong to the airframe are extracted from the mode shape matrix $\boldsymbol{\Phi}^{\mathrm{CS}} = [\boldsymbol{\phi}_1^{\mathrm{CS}}, \ldots, \boldsymbol{\phi}_{n^{\mathrm{CS}}}^{\mathrm{CS}}]$ with a selector matrix $\boldsymbol{T} \in \mathbb{R}^{n^{\mathrm{A}}\times n^{\mathrm{CS}}}$ so that $\hat{\boldsymbol{\Phi}}^{\mathrm{A}} = \boldsymbol{T}\boldsymbol{\Phi}^{\mathrm{CS}}$. However, in $\hat{\boldsymbol{\Phi}}^{\mathrm{A}}$ there are also modes included where (almost) only the rotor blades oscillate. It is not possible to approximate these modes with a surrogate mass and these modes are also not relevant for the investigation of the dynamical behavior of the airframe. Thus, these pure rotor blade modes are filtered out by normalizing each airframe mode shape with the maximal oscillation amplitude of mode shape of the coupled system

$$\hat{\boldsymbol{\phi}}_i^{\mathrm{A,nom}} = \frac{\hat{\boldsymbol{\phi}}_i^{\mathrm{A}}}{\max(\boldsymbol{\phi}_i^{\mathrm{CS}})}, \quad i = 1, 2, \ldots, n^{\mathrm{CS}}. \tag{18}$$

Now, only those modes are kept, where the maximum of the normalized eigenvector exceeds a given threshold. A threshold of 0.1 leads to reasonable results and is used in the following. In this way, only those modes are kept in the mode shape matrix $\boldsymbol{V}_{\mathrm{A}}$, where the maximal elastic displacement of the airframe is at least 10% of the displacement of the rotor. Furthermore, those modes, where the airframe oscillates as a rigid body with the rotor are removed. The resulting

reference modes $\boldsymbol{\Phi}^{\mathrm{A,ref}}$ are visualized in Figure 2 on the right side and compared to the full mode shape matrix $\hat{\boldsymbol{\Phi}}^{\mathrm{A}}$. In both plots, the MAC between the coupled model and the free airframe model is shown. Higher MAC values indicate a better correspondence and are represented by darker and larger squares. The left MAC contains many modes of the coupled model that are not included in the free airframe modes and there is also no chance to approximate these modes by adding a single surrogate mass. The reference mode shapes remaining in the right MAC do not exactly coincide with the free airframe model but, the similarity is recognizable. These modes are intended to be approximated by optimizing the lumped mass of the surrogate model.

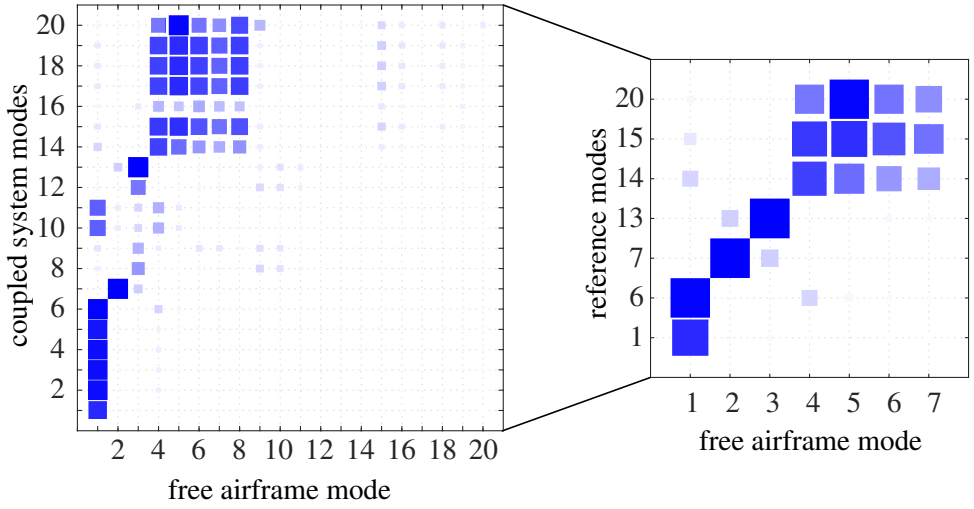

Figure 2: Modal assurance criterion for unfiltered coupled system modes left and selected relevant reference modes right compared to the first free airframe modes.

4 SURROGATE MODEL FITTING

In this section, the approach to tune a surrogate mass that substitutes the rotor and approximates the vibrational behavior of the coupled system is described. A lumped mass is attached to the rotor and the amount of the mass m is the optimization variable which is tuned to fit the reference model.

4.1 Reduced parametric model formulation

The first step is the formulation of an affine parametric model with linear regression. This model can be reduced using PMOR methods, which is necessary to allow for many system evaluations in a reasonable time. The reduced model has the form

$$\begin{aligned} \left[\tilde{\boldsymbol{M}}_0 + \tilde{\boldsymbol{M}}_1(m)\right]\ddot{\tilde{\boldsymbol{q}}} + \tilde{\boldsymbol{K}}\tilde{\boldsymbol{q}} &= \tilde{\boldsymbol{B}}\boldsymbol{u}, \\ \tilde{\boldsymbol{y}} &= \tilde{\boldsymbol{C}}\tilde{\boldsymbol{q}}. \end{aligned} \tag{19}$$

The approach that seems straightforward to approximate the eigenmodes is modal truncation. However, when generating local modal bases for different m and unifying all local subspaces to one global basis, the singular values

$$\sigma_i \quad \text{with} \quad \boldsymbol{V}_{\mathrm{G}} = \boldsymbol{U}\boldsymbol{\Sigma}\boldsymbol{D}, \quad i = 1,\ldots,n_G \quad \text{and} \quad \boldsymbol{\Sigma} = \mathrm{diag}(\sigma_{\mathrm{i}}) \tag{20}$$

decay very fast. In Figure 3 the local bases at each parameter point are spanned by 80 vectors. For the modal truncation, the singular values drop drastically after the 80th singular value while for Krylov reduction they decay only slowly. This is because the Krylov subspace method can capture the parameter dependency better and subspaces at different parameter samples add information to the reduced system so that the singular values decay slower. Since the preservation of the parameter dependence is very important for the optimization, the Krylov method is suited better here.

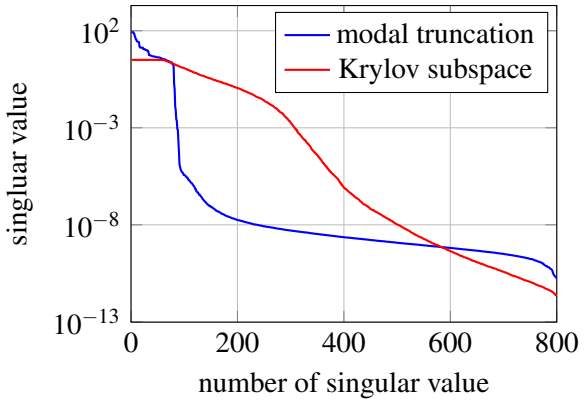

Figure 3: Decay of singular values for PMOR using modal truncation and the Krylov subspace method.

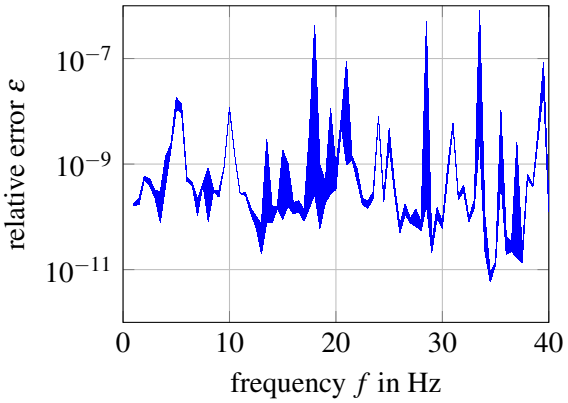

Figure 4: Relative error range for 100 transfer function evaluations at randomly picked parameter points.

By using the Krylov subspace method with 10 equidistant parameter points in the considered range of $m \in [0, 2m^{\mathrm{R}}]$, where m^{R} is the actual rotor mass, and equidistantly distributed shifts in the frequency range of $[0,40]$Hz, a reduced order model of size $n_{\mathrm{G}} = 800$ is generated that captures the parametric behavior of the full system very well. Figure 4 shows the relative error of the transfer behavior for characteristic inputs and outputs. The error is evaluated at 100 random parameter values and the resulting error range is shown. The relative transfer function error never exceeds 10^{-6} and eigenmodes and eigenfrequencies match almost exactly with those of the full model. Thus, this model is well-suited for optimization.

4.2 Objective function

The objective function should ensure the correspondence of mode shapes as well as the correspondence of eigenfrequencies between the reference model and the reduced parametric model. In [16] the objective function

$$\varepsilon(m) = \sum_{i=1}^{n_{\mathrm{f}}} \left[\left(\frac{f_{\mathrm{ref},i} - f_i(m)}{f_{\mathrm{ref},i}} \right)^2 + \left(\frac{1 - \sqrt{\mathrm{MAC}_{ii}(m)}}{\sqrt{\mathrm{MAC}_{ii}(m)}} \right)^2 \right] \tag{21}$$

is used for the geometry optimization of guitars for the first n_{f} modes. It can also be used in a similar form here to find the most appropriate surrogate mass for the vibration test of the helicopter. As Figure 2 reveals, the surrogate modeling cannot approximate the entire behavior of the coupled system. One can see, that the first reference mode, e.g, is not well described by the surrogate model. This does not change significantly with a changing mass m, as also Figure 5a shows. Here, the objective function is plotted for the difference between the first reference mode and the first mode of the surrogate model. The value decreases for an increasing mass but even for the boundaries, the error is still significant. The first mode is described by the tailboom moving up and down with flapping rotor blades. This behavior cannot be approximated with a single point mass. Not the entire behavior of the coupled system can be described with the reference model, but only certain modes. Furthermore, it is possible that the reference mode and the surrogate mode that correspond to each other do not have the same mode number. The objective function is, thus, modified to

$$\varepsilon_i^*(m, j) = \left(\frac{f_{\mathrm{ref},i} - f_j(m)}{f_{\mathrm{ref},i}} \right)^2 + \left(\frac{1 - \sqrt{\mathrm{MAC}_{ij}(m)}}{\sqrt{\mathrm{MAC}_{ij}(m)}} \right)^2 \tag{22}$$

which allows optimizing the surrogate mass for one given eigemomde i and changing the mode number j of the surrogate system during optimization. By introducing the second variable j, the

minimization of $\varepsilon_i^*(m,j)$ can no longer be solved deterministically, which is why a generic particle swarm algorithm is used to solve the problem under the boundaries $m \in [0, 2m^{\mathrm{R}}]$.

5 RESULTS

Solving the minimization problem

$$[m_{\mathrm{opt}}, j_{\mathrm{opt}}] = \arg \min_{m\in[0,2m^{\mathrm{R}}],\ j\in[1,n_{\mathrm{G}}]} \varepsilon_i^*(m,j) \tag{23}$$

for different eigenmodes, one can improve the validity of the surrogate model. Note that this optimization is only possible in a reasonable time because of the use of PMOR. An evaluation of the objective function takes slightly more than one second of CPU time on an Intel(R) Xeon(R) CPU E5-1650 v3 @ 3.50GHz processor for the reduced model while it takes more than six minutes for the full model, which is a speed-up with a factor greater than 280. In Figure 5, the deviation of eigenfrequencies, MAC and the objective function value is plotted over the surrogate mass for different modes. For the plots, the deviation is always computed for the mode j_{opt} which was identified to be the one with minimal deviation. As outlined in Subsection 4.2, there is no suitable mass to approximate the first eigenmode. However, for the two other examples, a minimum in the objective function is clearly visible. These are important modes because their frequencies lie closest to the first rotor harmonic frequency $f = {}^{1}/_{\mathrm{rev}}$ (Figure 5b) and to first blade passage frequency $f = {}^{5}/_{\mathrm{rev}}$ (Figure 5c) of the five-balded rotor. Interestingly, there is not one mass that fits all modes but the optimization yields different results for different mode shapes. While for the eigenmode closest to the rotor harmonic the best approximation is reached for $m_{\mathrm{opt}} = 0.95m^{\mathrm{R}}$, a mass of $m_{\mathrm{opt}} = 0.25m^{\mathrm{R}}$ is found for the eigenmode closest to the blade passage frequency. Note that the minimum of the MAC and the eigenfrequency do not always match exactly. Indeed, there is a significant difference for some modes, e.g., in Figure 5b. However, the accordance of the MAC is here good over the whole parameter region with deviations smaller than 1% which ensures that the same mode shapes are compared.

When optimizing the first modes separately and comparing the eigenmodes to the reference modes, one can find the improved MAC shown in Figure 6. It is visualized that the accordance between the coupled reference system and the free airframe can be improved significantly by adding an optimal mass for the given eigenmode.

6 CONCLUSION

A novel approach to determine a surrogate mass for helicopter ground vibration tests was introduced which aims at representing the main rotor. A reduced order surrogate model was built which has relative errors in the transfer behavior smaller than 10^{-6} and accelerates the evaluation of the objective function by a factor of 280. By optimizing the modal assurance criterion and the eigenfrequencies, optimal surrogate masses were found that do not necessarily correspond to the actual rotor weight. It was shown, that the surrogate system can approximate the coupled reference better when attaching these optimal masses. In future work, modal in-flight test data can be used as a reference solution to further improve the validity of the surrogate model and also the surrogate model itself can be extended, e.g., with surrogate mass systems instead of just one lumped mass.

Acknowledgments

This research is performed within the framework of the EVOLVE research project (FKZ 20A1902C) funded by the German Federal Ministry for Economic Affairs and Climate Action. This support is highly appreciated.

Supported by:

Federal Ministry
for Economic Affairs
and Climate Action

on the basis of a decision
by the German Bundestag

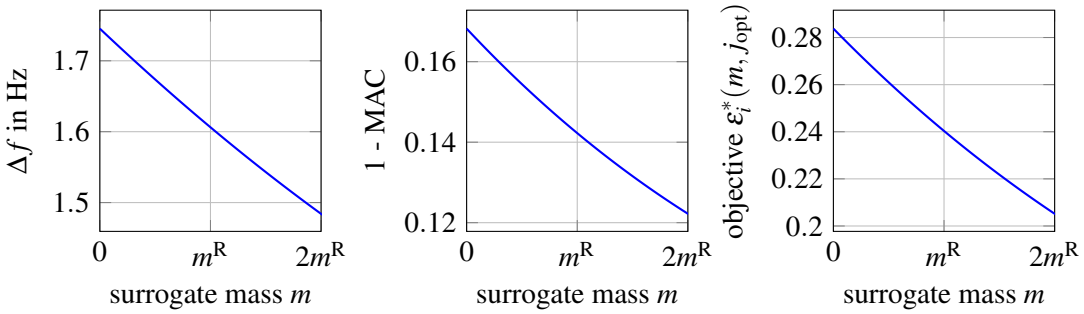

(a) First eigenfrequency of the coupled system

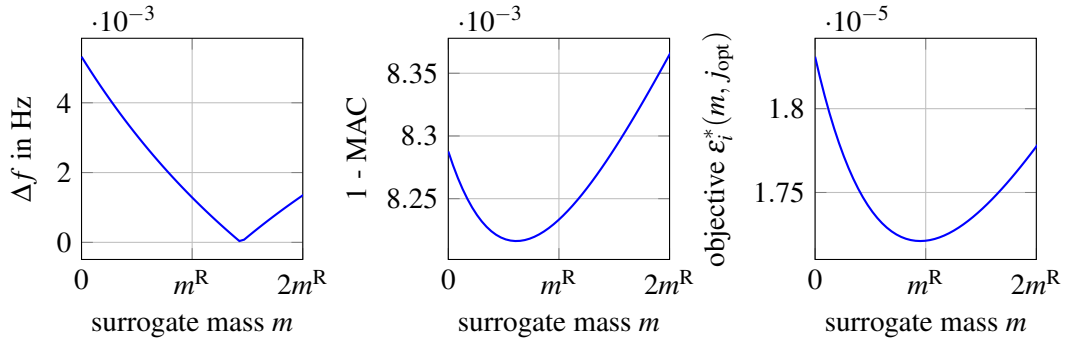

(b) Eigenmode closest to first rotor harmonic frequency

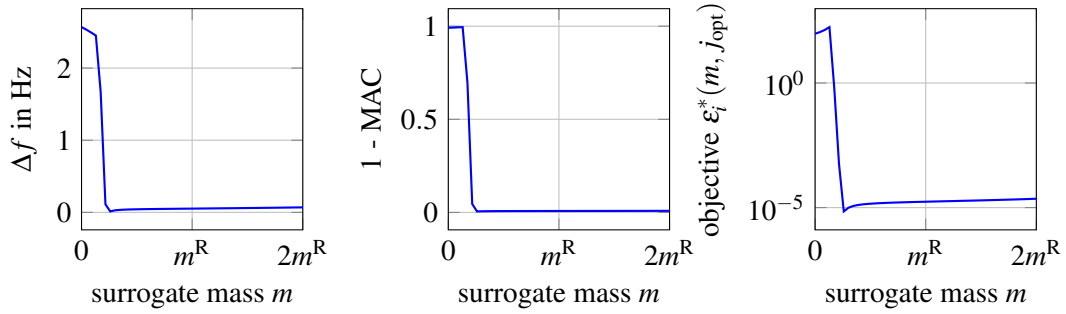

(c) Eigenmode closest to blade passage frequency

Figure 5: Deviation between the reduced surrogate model and the reference model, and progress of objective function for three different eigenmodes of the system.

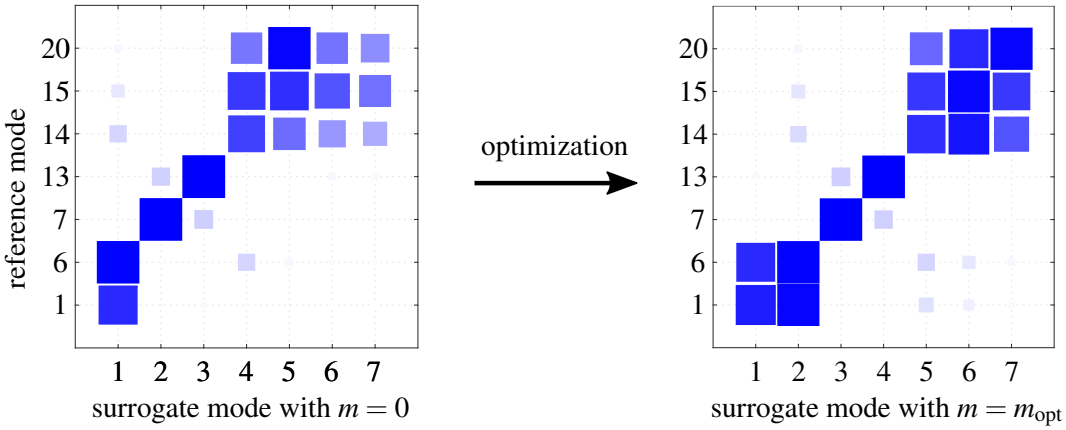

Figure 6: Comparison of MAC between the reference model and the surrogate model for $m = 0$ and $m = m_{opt}$.

REFERENCES

[1] Ciavarella, C., Priems, M., Govers, Y., Böswald, M.: An extensive helicopter ground vibration test: from pretest analysis to the study of non-linearities. In: Proceedings of the 44th European Rotorcraft Forum, Delft, Netherlands. (2018)

[2] Shabana, A.A.: Dynamics of Multibody Systems. Cambridge University Press, New York (2005)

[3] Wallrapp, O.: Standard Input Data of Flexible Bodies for Multibody System Codes. Report IB 515-93-04, DLR, German Aerospace Establishment, Institute for Robotics and System Dynamics, Oberpfaffenhofen (1993)

[4] Schwertassek, R., Wallrapp, O.: Dynamik flexibler Mehrkörpersysteme (in German). Vieweg, Braunschweig (1999)

[5] Weiß, F., Merlis, J., Lojewski, R., Hofmann, J., Röhrig-Zöllner, M.: Rotor blade modeling in a helicopter multi body simulation based on the floating frame of reference formulation. In: Proceedings of the 44th European Rotorcraft Forum, Winterthur, Switzerland. (2022)

[6] Frie, L., Dieterich, O., Eberhard, P.: Model order reduction for elastic multibody systems with fast rotating bodies. In: ECCOMAS Thematic Conference on Multibody Dynamics, Budapest, Hungary. (2021) 432–443

[7] Frie, L., Dieterich, O., Eberhard, P.: Parametric model order reduction for speed-controlled elastic rotors. In: Proceedings of ISMA2022, Leuven, Belgium. (2021) 2110–2122

[8] MSCSoftware: MSC Nastran 2012 – Quick Reference Guide. (2011)

[9] Antoulas, A.: Approximation of Large-Scale Dynamical Systems. SIAM, Philadelphia (2005)

[10] Fröhlich, B., Hose, D., Dieterich, O., Hanss, M., Eberhard, P.: Uncertainty quantification of large-scale dynamical systems using parametric model order reduction. Mechanical Systems and Signal Processing **171** (2022) 108855

[11] Gugercin, S., Antoulas, A.C., Beattie, C.A.: $\mathscr{H}_2$ Model reduction for large-scale linear dynamical systems. SIAM Journal on Matrix Analysis and Applications **30**(2) (2008) 609–638

[12] Frie, L., Eberhard, P.: On shift selection for Krylov subspace based model order reduction. Multibody System Dynamics (2023) 1–21

[13] Baur, U., Beattie, C., Benner, P., Gugercin, S.: Interpolatory projection methods for parameterized model reduction. SIAM Journal for Scientific Computing **33**(5) (2011) 2489–2518

[14] Craig, R., Bampton, M.: Coupling of substructures for dynamic analyses. AIAA Journal **6**(7) (1968) 1313–1319

[15] Hasbun, M., Saberi, H., Blumenstein, R.: Modal elastic component enhancements for RCAS. In: Proceedings of the VFS International 76th Annual Forum & Technology Display, Virginia, USA. (2020)

[16] Brauchler, A., Ziegler, P., Eberhard, P.: An entirely reverse-engineered finite element model of a classical guitar in comparison with experimental data. The Journal of the Acoustical Society of America **149**(6) (2021) 4450–4462